JCI insight

Gonadotrope androgen receptor mediates pituitary responsiveness to hormones and androgen-induced subfertility

Zhiqiang Wang, … , James Segars, Sheng Wu

JCI Insight. 2019. https://doi.org/10.1172/jci.insight.127817.

Research In-Press Preview Endocrinology Reproductive biology

Graphical abstract

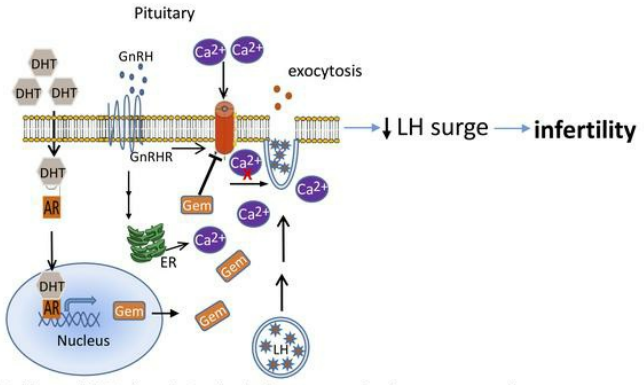

Working model. We hypothesize that in the presence of androgen excess, androgen receptor (AR) binds to DHT and increases *Gem* mRNA level. GEM inhibits calcium influx by blocking voltage-dependent calcium channel (VDCC). GnRH binds its receptor (GnRHR) to induce release of LH by stimulating vesicle exocytosis. Reduced cytosolic Ca2+ concentration due to increased GEM inhibits Ca2+ triggered exocytosis, reducing LH vesicle secretion during GnRH stimulation, therefore DHT reduces LH surge and impairs reproductive function. ER: endoplasmic reticulum.

Gonadotrope Androgen Receptor Mediates Pituitary Responsiveness to Hormones and Androgen-Induced Subfertility

Zhiqiang Wang[1], Mingxiao Feng[1], Olubusayo Awe[1],Yaping Ma[1,5], Mingjie Shen[1,6], Ping Xue[1], , Rexford Ahima[4], Andrew Wolfe[1,2], James Segars[3], Sheng Wu[1,2,3]*

[1]Department of Pediatrics, Johns Hopkins University School of Medicine, Baltimore, MD, 21087

[2]Department of Molecular and Cellular Physiology, Johns Hopkins University School of Medicine, Baltimore, MD, 21087

[3]Department of Gynecology and Obstetrics, Johns Hopkins University School of Medicine, Baltimore, MD, 21287

[4]Department of Medicine, Johns Hopkins University School of Medicine, Baltimore, MD, 21287

[5]Department of Pediatrics, Affiliated Hospital of Jiangnan University, Wuxi, Jiangsu, 214062, P.R. China

[6]Department of Gynecology and Obstetrics, Shuguang hospital affiliated to Shanghai University of Traditional Chinese Medicine, Shanghai, 201203, P.R. China

* Correspondence and name of person to whom reprint requests should be addressed:

Sheng Wu

600 North Wolfe Street, CMSC-406

MD, USA 21287

Tel +1 410-5027573

Fax 410-5027580

Email : swu24@jhmi.edu

The authors have declared that no conflict of interest exists

Abstract

Many women with hyperandrogenemia suffer from irregular menses and infertility. However, it is unknown whether androgens directly affect reproduction. Since animal models of hyperandrogenemia-induced infertility are associated with obesity, which may impact reproductive function, we have created a lean mouse model of elevated androgen using implantation of low dose dihydrotestosterone (DHT) pellets to separate the effects of elevated androgen from obesity. The hypothalamic-pituitary-gonadal axis controls reproduction. While we have demonstrated that androgen impairs ovarian function, androgen could also disrupt neuroendocrine function at the level of brain and/or pituitary to cause infertility.

To understand how elevated androgens might act on pituitary gonadotropes to influence reproductive function, female mice with disruption of the androgen receptor (*Ar*) gene specifically in pituitary gonadotropes (PitARKO) were produced. DHT treated control mice with intact pituitary *Ar* (Con-DHT) exhibit disrupted estrous cyclicity and fertility with reduced pituitary responsiveness to GnRH at the level of both calcium signaling and LH secretion. These effects were ameliorated in DHT treated PitARKO mice. Calcium signaling controls GnRH regulation of LH vesicle exotocysis. Our data implicated upregulation of GEM (a voltage-dependent calcium channel inhibitor) in the pituitary as a potential mechanism for androgen's pathological effects. These results demonstrate that gonadotrope AR, as an extra-ovarian regulator, plays an important role in reproductive pathophysiology.

Keywords: Androgen, PCOS, Reproduction, Pituitary, Estrous cycling, LH, Gem

Introduction

Hyperandrogenemia is a salient feature in many women who suffer irregular menses, oligo/anovulation and infertility, including women with polycystic ovary syndrome (PCOS)(1), classic and non-classic (late-onset) congenital adrenal hyperplasia (CAH)(2-5), exogenous testosterone treatment in female to male transsexuals(6-10), exogenous androgen use (body builders), or environmental toxicity(11). Although each of these conditions feature androgen excess, in some cases (e.g. PCOS), it is not clear whether increased androgen levels are a consequence of reproductive pathology, or directly contribute to the progression of reproductive pathology.

Several models have been developed in rodents and other animals to probe the effects of androgens on the reproductive axis (4,12),(13-17). These models showed reproductive dysfunction, but were also associated with obesity. This is problematic because obese female rodents and women have higher circulating testosterone levels and impaired fertility (18-20). Consequently, it is not possible determine whether the phenotype is caused by the androgen excess or obesity. To address this problem, we created an adult mouse model(21-23) that develops reproductive and metabolic dysfunction within two weeks after chronic DHT exposure from a pellet containing DHT (2xDHT mice). This model produces serum DHT levels in mice that are 2-fold higher than in controls. Importantly, the mildly elevated levels resemble the 1.5 to 3.9 fold elevation of testosterone and DHT in women with PCOS(4,24-30). Notably, the 2xDHT mice do not exhibit alterations of basal serum estradiol, testosterone, LH and do not develop obesity, and show similar ovarian weight, serum levels of cholesterol, free fatty acids, leptin, TNFα and IL-6 relative to controls even up to 3.5 months after DHT insertion(21,22,31).

Due to the interconnected nature of the hypothalamic-pituitary-gonadal axis, effects of excess androgens could be exerted at multiple levels of the axis (22,32). While some androgen effects occur in the brain, as reported by others (32,33), whether ARs in gonadotropes contribute to the

dysregulation of female estrous cycles and gonadotropin secretion is unknown. To define how androgen/AR in the pituitary contributes to reproductive dysfunction, and the molecular mechanisms are underlying the pathophysiology, we used the 2X DHT mouse model with intact (Control; $AR^{fl/fl}$, Cre^{-}) or disrupted AR in gonadotropes (PitARKO; $AR^{fl/fl}$, $Cre^{+/-}$)(34) to probe the role of AR in gonadotrope cells (Figure 1). Since pituitary responsiveness to GnRH stimulation is disrupted by high androgens (35) *in vitro*, and because GnRH-mediated increases in cytosolic Ca^{2+} are crucial for exocytosis of LH granules (36,37), we studied GEM, a GTP-binding protein that binds calmodulin to reduce Ca^{2+} influx (36-38). Our findings demonstrate important roles for gonadotropic AR in reproduction as an extra-ovarian regulatory factor. Gonadotropic AR mediated reproductive dysfunction may act through GEM, reducing LH secretion from the pituitary in the presence of DHT.

Results:

DHT disrupts estrous cyclicity in control but reserved in PitARKO mice

To explore the role of pituitary AR in hyperandrogenic induced abnormal cyclicity, we analyzed four groups of mice (control-no DHT (Con-no DHT), Con-DHT, PitARKO-no DHT and PitARKO-DHT). Since PitARKO mice bore reduced number of pups compared to control littermates under normal androgen conditions(34), we compared reproductive physiology in mice with the same genotype as described (32). As expected, we observed that Con-DHT mice spent significantly less time in proestrus (P) and estrus (E) phases and more time in diestrus (D) and metestrus (M) than Con-no DHT mice (Figure 2A-B). The time in proestrus of PitARKO-DHT mice was approximately 70% compared to Con-no DHT mice without a significant reduction compared to PitARKO-no DHT. In PitARKO-DHT mice estrous cyclicity was virtually indistinguishable from PitARKO-no DHT mice.

Androgen-induced fertility impairment was reduced in PitARKO mice

Pups and litters per dam were recorded during 90 days of mating and displayed as a fertility plot (for brevity, only fertility plots from PitARKO-DHT and Con-DHT groups are shown; Figure 3A). Fertility data from all four groups was further analyzed to assess total number of litters and pups per female. The number of litters (Figure 3B) and pups per female (Figure 3C) were both significantly reduced in control mice treated with DHT (Con-DHT vs Con-no DHT). While the number of litters from PitARKO-DHT mice were reduced, the reduction in litter size was significantly greater than the Con-no DHT mice. Also, the number of pups was reduced when compared to Con-no DHT, but the reduction was not significant compared to PitARKO-no DHT mice. Importantly, the number of litters and pups was significantly higher in PitARKO-DHT mice compared to Con-DHT mice (Figure 3B and C) which suggests that *Ar* knockout in gonadotropes partially mitigated the impairment in fertility caused by androgens. As we have previously reported, under normal androgen levels, PitARKO mice have a similar number of litters compared to control mice while the number of pups was significantly reduced (Figure 3 and(34)).

Androgen-induced disruption of ovulation was mitigated in hyperandrogenic mice lacking gonadotropic AR

Morphology of representative ovaries from Con-no DHT, Con-DHT, PitARKO-no DHT and PitARKO-DHT mice is shown in Figures 3D-G. A marked difference was difference in abundance of CLs (corpora lutea) that serves as an anatomical marker of recent ovulation. CLs were much less common in the ovaries of the Con-DHT mice than in any of the other three groups (Figure 3D-H). Con-DHT ovaries had significantly fewer CLs compared to ovaries from Con-no DHT mice. However, the number of CLs in PitARKO-DHT ovaries were not significantly different from ovaries from PitARKO-no DHT females.

Pituitary responsiveness to GnRH stimulation was preserved in PitARKO-DHT mice

To investigate the effects of DHT on pituitary responses to GnRH, control and PitARKO female mice, with or without DHT, were stimulated with GnRH and LH levels were analyzed. While all four groups had the same basal levels of LH (Figure 4A), following GnRH stimulation the Con-DHT mice had a significantly attenuated LH release when compared to Con-no DHT mice. In contrast, both PitARKO-no DHT and PitARKO-DHT had levels of LH release indistinguishable from one another or Con-no DHT mice. As expected, FSH levels were not altered 20 minutes after GnRH treatment across all 4 groups (Figure 4B). Similar responses were observed *ex vivo*. Cultured primary pituitary cells from control (ARfl/fl; Cre-) mice were treated with DHT for 42 hrs. LH and FSH secretion into the media was measured from these cells following treatment for 2h with GnRH. LH and FSH secretion following GnRH stimulation was reduced in a dose responsive manner when treated with 1nM or 10nM DHT compared to no DHT treatment (Figure 4C-D). Further, DHT did not inhibit GnRH stimulated LH secretion in cultured pituitary cells of PitARKO mice (Suppl. Figure 3). These *ex vivo* data suggest that DHT through AR attenuates pituitary responsiveness to GnRH.

PitARKO abolished DHT-induced upregulation of *Gem* expression to potentiate LH secretion in response to GnRH stimulation

To further investigate the mechanisms by which AR causes DHT-induced loss of pituitary responsiveness, we examined pituitary mRNA expression *ex vivo* in cultured pituitaries from control mice. We observed that *Lhb* mRNA levels were significantly reduced 42 hr after DHT treatment. However, *Gem* transcripts, an inhibitor of voltage-dependent calcium (Ca^{2+}) channels, were upregulated following DHT treatment (Figure 4E-F). We then examined RNA expression *in vivo*, harvested from pituitaries of each of the four groups of mice. We confirmed that *Ar* mRNA expression in pituitary was significantly lower in PitARKO mice compared to control mice with or without DHT (with normal *Tshβ* mRNA(34)). *Lhb* mRNA was not significantly different between groups, which differed from the results obtained from the *ex vivo* model (Figure 4E-H).

However, in concordance with the *ex vivo* model, *Gem* was upregulated upon DHT treatment in pituitaries from Con-DHT compared to no-DHT treated mice, while PitARKO mice did not have DHT-induced upregulation of *Gem* (Figure 4I).

Calcium signaling in response to GnRH stimulation was preserved in pituitaries from PitARKO mice

Inhibition of Ca^{2+} channels by GEM reduces Ca^{2+}-triggered exocytosis in hormone-secreting cells. This is true for LH secretion from gonadotropes which requires exocytosis, a process highly dependent on intracellular calcium concentration. To investigate whether DHT treatment inhibits Ca^{2+} concentration via AR signaling in the pituitary, we performed intracellular calcium kinetics assay using *ex vivo* primary pituitary cells. We observed that DHT treatment dramatically inhibited the intracellular calcium rise in control pituitaries in response to 50nM GnRH stimulation compared to non-DHT treated pituitaries. Pituitary cells from PitARKO mice exhibited similar intracellular calcium increases regardless of DHT treatment following 50nM (Figure 5A-B) or 10nM (data not shown) GnRH stimulation. These results are consistent with our observation that DHT treatment can upregulate *Gem* and diminish LH secretion in response to GnRH stimulation.

AR binds to the promoter of *Gem* and increases Gem promoter expression

In order to examine if AR directly binds the promoter of the *Gem* gene to regulate transcription, we scanned a 5000bp region of the *Gem* promoter and found two putative consensus binding sites for AR (ARE). Chromatin immunoprecipitation (ChIP) was performed to validate AR binding to these elements. As shown in Figure 5C-E, DHT treatment significantly increased occupancy of AR on *Gem* promoter binding site 1 (between -607 and -593 (tagcacaagctgctt)); and an increase (though not significant) in occupancy on *Gem* promoter binding site 2 (between -510 and -496 (tgggacatactgctt)). There was almost no detectable AR binding to the *Gem* promoter in pituitaries of PitARKO-DHT mice (Figure 5F) after immunoprecipitation. AR is mainly expressed in gonadotropes(39,40). Although gonadotropes only occupy 10% of pituitary cells, PitARKO mice showed more than 50% reduction of AR expression(34). Further, DHT treatment significantly increased *Gem* promoter luciferase expression compared to empty vector as shown in Figure 5G.

Discussion

Several lines of evidence indicate that pituitary responsiveness to GnRH stimulation is disrupted by testosterone (35,41,42). Foecking et al., demonstrated that DHT treatment led to suppression of LH surges and basal LH secretion. When we used 10nM DHT *ex vivo*, levels used by Foecking et al.(41,42), we also observed reduced basal LH secretion in control mice. Further, testosterone has been shown to suppress LH and FSH secretion independent of peripheral aromatization in both men(43-45) and women(9,43). Although LH is often elevated in women with PCOS and in non-rodent animal models of PCOS, this could be due to the timing of androgen exposure, adult versus gestational androgen exposure, and not the species differences. This indicates that although species differences exist in the neuroendocrine regulation of ovulation, DHT reduces pituitary responsiveness to GnRH in both animal models and in humans. One explanation is that acquired androgen excess (DHT treatment in adult females) may be fundamentally different from developmental exposure to androgen excess regarding LH secretion, such as PCOS, which often show increased LH pulse frequency, and enhanced pituitary response to GnRH stimulation(46). Women with elevated androgen frequently present with disrupted gonadotropin secretion(17), and confirming a role for AR, women with PCOS (or PCOS-like model in rodent) have recovered ovulation after long-term treatment with the competitive AR antagonist, flutamide(18,47-51). Further, although anovulatory women with PCOS have higher basal levels of LH, LH surge is indeed inadequate. These females did not show any LH surges during 40 days of monitoring and LH surges were only restored after long-term flutamide treatment(18). Collectively, clinical observations, animal models and pharmacological studies have provided strong evidence to support the direct involvement of elevated androgen, and its receptor (AR) in mediating actions of dysregulated female reproductive physiology (52-54). Understanding how androgen/AR affects reproduction through animal models is important for developing improved clinical interventions for treating reproductive dysfunction.

Female mice exhibit a two fold increase in testosterone levels compared to basal levels during the preovulatory surge(34) and this has been shown to be required for normal rates of ovulation, however, higher chronic doses of androgens reduce rates of ovulation(55). Serum androgen levels in women with PCOS or women with corrected congenital adrenal hyperplasia (CAH) are approximately 2-3 fold higher than in normal women(4,56,57). Because of this, and in contrast to other models, we created a model with DHT insertion which produces serum androgen levels that are approximately two-fold higher than in untreated mice. In general, female testosterone levels are very low and therefore the DHT levels are also very low. The circulating DHT levels in our DHT-treated mice were two-fold higher than untreated mice, suggesting that the pituitary in DHT treated mice were also exposed to two-fold higher DHT levels than untreated mice. Women with PCOS have higher levels of circulating androgens, and it is logical to expect that higher DHT levels would be found in tissues that have 5-alpha-reductase. The 2xDHT levels *in vivo* may not reflect the highest levels of DHT in pituitary. However, the 10nM DHT level we used *ex vivo* is comparable to male levels of DHT, and may result in levels much higher than achieved with *in vivo* treatment.

Dissecting the effects of AR in the pathophysiology of elevated androgen is complicated and difficult using approaches that involve global AR KO. Because AR is widely expressed in different tissues and cell types, the extent to which circulating androgens impact these tissues and contribute to observed reproductive effects remains unclear. Mice with conditional AR knockouts have helped to define the tissue-specific mechanism of action of androgen signaling. Females with ovarian theca ARKO (ThARKO) exhibit normal reproductive function under normal androgen conditions(22). However, ThARKO-DHT mice showed improved estrous cyclicity, ovulation and fertility compared to Con-DHT mice, though function was not equivalent to wild type or ThARKO females without DHT(22). Central nervous system AR knockout mice showed normal reproductive function(32) (and our unpublished data) under normal androgen conditions. However, under conditions of androgen excess these mice still exhibited aberrant cyclicity and only had a partial

mitigation of DHT-induced reductions in CL(32,58). Therefore, these studies do not explain the entirety of the reproductive dysfunction caused by DHT.

We previously reported that the expression of AR (both protein and mRNA) in ovary is the same between control and PitARKO mice(34). Consistent with previous findings from our laboratory(34), in the absence of elevated androgen, PitARKO female mice are fertile, although they did have fewer pups per litter than controls. In the presence of high androgen levels, control mice became acyclic and infertile while PitARKO mice, like ThARKO mice, exhibited reduced acyclicity and infertility compared to Con-DHT. However, PitARKO-DHT mice had only a partial reduction in infertility since these mice still showed reduced litters compared to both PitARKO-no DHT and Con-no DHT, reduced pups compared to Con-no DHT (Figure 3B-C). PitARKO-DHT mice also showed reduced time (length) of Proestus than PitARKO-no DHT, although the reduction was not significant. The time of proestrus in PitARKO-DHT mice is roughly 70% of that compared to Con-no DHT mice. Therefore, deletion of ARs in either gonadotropes or theca cells only partially mitigated the adverse effects of androgens on fertility and cyclicity. These observations demonstrate ARs in pituitary gonadotropes play a vital role in hyperandrogenemic-induced infertility and further demonstrates that each component of the H-P-G axis contributes to hyperandrogenemia induced reproductive dysfunction(32,34).

Gonadotropes located in the anterior pituitary secrete LH and FSH following GnRH stimulation. We observed hyperandrogenemia did not affect basal LH levels *in vivo*. However, under hyperandrogenemic conditions, while Con-DHT mice showed reduced LH secretion in response to GnRH, PitARKO mice did not exhibit attenuated LH levels (Figure 4A). Therefore, deletion of AR in gonadotropes preserved LH secretion and pituitary responses to GnRH in hyperandrogenized adult mice. Although GnRH analog-stimulated LH release was only modestly impaired by DHT in control mice (Figure. 4A), and that large amplitude LH surges are not required for ovulation in mice, we suspect there is a threshold for LH stimulated ovulation, and the number of eggs to be released is partially controlled by the amplitude of LH in DHT treated mice. As

previously reported(22), LH receptor expression is reduced in ovary after DHT treatment; therefore, the ovary may be less responsive to LH stimulation (or less sensitive due to reduced LH receptor and or other factors). LH levels may not have reached the threshold for ovulation in Con-DHT mice compared to Con-no DHT mice. This interpretation is supported by our new data with superovulation regimen. DHT treated mice released significantly fewer eggs compared to no DHT treated mice after 5 units of hCG, consistent with the conclusion that the ovary is less responsive to LH stimulation. However, DHT treated mice with 10 units of hCG released an identical number of eggs compared to no DHT treated mice, further demonstrating that the amplitude of LH is important for ovulation (Suppl. Figure 1).

In female mice, the gonadotropic LH surge stimulates ovulation, which is an essential process in fertility and is induced by positive feedback of estradiol on the hypothalamus and pituitary. To explore whether positive feedback regulation was disrupted by DHT in our model like observed in rat(42), we used a surge induction paradigm that produced LH surge generation within 1 h before lights off (8pm) on the next day of estradiol injection. As observed before(59), LH levels at 10am and 9pm were low at values similar to the basal level of mice before OVX (data not shown). Therefore, the LH levels at 10 am were used as the baseline. We observed reduced LH surges in Con-DHT mice compared to Con-no DHT and PitARKO-DHT mice (Suppl. Figure 2) at 8pm. Given that pituitary responsiveness is a prerequisite for ovulation, DHT-induced attenuation of the LH secretion and reduced sensitivity of ovary to LH may explain why there were fewer CL in adult Con-DHT mice.

Androgens can act on the brain and pituitary to influence pituitary function directly or indirectly. Furthermore, there are complex positive and negative feedback loops involving the ovary at both the hypothalamus and pituitary levels that influence gonadotropin secretion. To avoid these issues and directly assess androgen effects by AR in gonadotropes, we tested androgen/AR mediated actions in isolated pituitary cultures obtained from control mice. As shown *in vivo* (Figure 4A), e*x*

vivo primary pituitary cultures confirmed that chronic androgen treatment decreased LH secretion in response to GnRH stimulation (Figure 4C); however, DHT did not reduce LH secretion after GnRH stimulation in PitARKO mice (Suppl, Figure 3). We observed that *Lhβ* expression was significantly reduced in DHT treated primary cultured pituitaries compared to vehicle treated pituitaries *ex vivo,* but not *in vivo*. This may be due to the action of other factors *in vivo* that interfere with DHT effects on the *Lhβ* expression.

LH secretion is controlled by Ca^{2+} influx ($[Ca2+]_i$) and mobilization. Spontaneous Ca^{2+} transients depend exclusively on Ca^{2+} influx through plasma membrane channels in gonadotropes and short (10-100 ms) depolarization of cell membrane does not trigger Ca^{2+} release from intracellular stores. Thus, the rise in $[Ca^{2+}]_i$ in spontaneously active pituitary cells exclusively depends on voltage-dependent Ca^{2+} channel (VDCC)(60). We found *Gem* was upregulated while KO of AR in gonadotropes abolished DHT-induced upregulation of *Gem* (Figure 4I, which was first identified by RNA-Seq, data not shown). Both extra- and intracellular calcium pools participate in GnRH-induced elevation of [Ca2+]i and LH secretion. Blocking plasma membrane calcium channel, decreased the magnitude of the Ca2+ current and reduced the plateau phase of LH release by 50%. Without extracellular Ca2+, the GnRH-induced [Ca2+]i peak was reduced and the plateau phase of increased Ca2+ concentration was abolished. GnRH stimulated calcium spikes and LH secretion are dependent on both the extracellular Ca2+-independent and extracellular Ca2+dependent (influx) phase. Voltage gated calcium entry is required for sustained agonist induced Ca2+ spiking and LH secretion(61). Therefore, reduction in calcium signaling cause by DHT could be due to reduced calcium influx and or impaired calcium mobilization. The reduction of the calcium spike following GnRH stimulation in hyperandrogenized control pituitaries resulted in reduced LH release, while hyperandrogenized pituitary cells from PitARKO mice exhibited a Ca2+ spike and LH secretion similar to non-DHT treated cells (Figure 5A-B). While the PitARKO mouse model allows for isolation of effects of pituitary AR from other tissues in DHT induced reproductive physiology, tissue specificity of androgen's effects are further confirmed by our *ex*

vivo studies in isolated pituitary cell preparations. When we measured calcium signaling in pituitaries from mice treated with DHT for 6 weeks, differences in calcium signaling were only present after GnRH dosages were 10 nM or higher (50nM). According to another report, differences in LH secretion was the greatest between vehicle and DHT treated cultured pituitary cells when GnRH concentrations were between 10nM to 100nM(62). Therefore, we used 50nM GnRH in this *ex vivo* experiment.

The AR is a member of the nuclear hormone family of transcription factors but can also mediate androgen action via non-nuclear mechanisms. Direct interactions with the *Gem* promoter were demonstrated by ChIP (Figure 5C-F), suggesting a direct transcriptional regulatory mechanism of action for AR mediated activation of *Gem* expression, that in turn may contribute to reduced calcium influx and reduced LH secretion. This finding highlights one molecular mechanism by which AR may contribute to regulation of LH secretion.

In summary, AR in gonadotropes contributes hyperandogenemia-induced reproductive dysfunction in adult mice. We propose that chronic hyperandrogenemia upregulates the VDCC inhibitor GEM which inhibits calcium influx in response to GnRH and decreases pituitary responsiveness, thus diminishing LH secretion causing anovulation and infertility (Figure 6).

Materials and Methods

Generation of hyperandrogenic females

PitARKO (ARfl/fl; aGSU driven cre+/-) mice and their controls (Cre-) were maintained in our laboratory, the same mouse line as previously described in a mixed background (C57/B6, CD1, and 129Sv)(34). To generate hyperandrogenic females, 2-month old adult females had subcutaneous insertion of an 8mm length pellet containing a 4-mm length of crystalline 5α-dihydrotestosterone (DHT) (DHT mice: Con-DHT; PitARKO-DHT) or an empty pellet (no-DHT mice: Con-no DHT; PitARKO-no DHT). To maintain the constant level of androgen excess in DHT females, DHT or no-DHT pellets were replaced every 4 weeks during the study (21-23,31,63). All experiments are conducted in female mice and all procedures were approved by the Johns Hopkins Animal Care and Use Committee.

Assessment of estrous cyclicity and reproductive phenotypes in hyperandrogenic females

To examine whether estrous cyclicity was disrupted equally in both control-DHT and PitARKO-DHT females, females implanted with DHT or an empty pellet were divided into two groups. Group1 was assessed for estrous cyclicity by assessing vaginal smear cytology for 16 consecutive days starting 3 days after DHT treatment. The stage of the estrous cycle was determined and classified as proestrus, estrus, and met/diestrus based on observed ratios of cornified epithelial, nucleated epithelial, and polymorphonuclear leukocytes as described in(64). The examiners were blinded to genotypes during all data collection.

Fertility was assessed in Group 2. Fifteen days after insertion of DHT or empty pellets, females were mated with proven fertile control males in monogamous manner. Pups and litter size from pregnant mice with and without DHT were recorded and counted for 90 days.

In vivo GnRH stimulation and hormone assays

LH secretion induced by GnRH is commonly used to assess pituitary function. To further investigate the roles of pituitary AR in hyperandrogenemia induced subfertility, following 6 weeks

of pellet insertion, GnRH analog (catalog no. L4513–1MG; Sigma-Aldrich) was injected subcutaneously at the nape of the neck at a dose of 200ng/kg body weight (BW) per mouse at diestrus between 9am to 10am. Whole blood was collected at 20 minutes after injection and luteinizing hormone (LH) and follicular stimulating hormone (FSH) were assayed by either Luminex assay (MPTMAG-49K, Millipore, Billerica, MA) or Ultra-Sensitive Mouse and Rat LH ELISA conducted by the Ligand Assay and Analysis Core, Center for Research in Reproduction at the University of Virginia (Charlottesville, Virginia).

Quantitative Real-Time PCR (qRT-PCR)

Pituitaries were isolated from mice at diestrus that had been treated with DHT or empty pellets for more than 6 weeks. Total RNA was extracted from the pituitaries by Trizol and reversed transcribed to cDNA with iScriptTM cDNA synthesis kit (Cat# 1708891, Bio-Rad) following the manufacturer's instructions. Messenger RNA transcripts of genes (*Lhb*, *Gem, Ar* and *Gapdh*) and *Gem* promoter gene expression were measured by qRT-PCR using iQSYBR green reagent according to the manufacturer's protocol (Bio-Rad). *Gapdh* was used as the internal control. Primers are listed in Table 1.

***Ex vivo* primary pituitary cell culture and GnRH stimulation**

Adult control or PitARKO mice without DHT insertion were sacrificed at diestrus by CO2 asphyxiation, decapitated and pituitaries collected. The pooled pituitaries (3-5 pituitaries) were washed with 10 ml of 10% FBS DMEM (Cellgro # 10-013-CV) at 2500 rpm for 5 min. Afterward the pituitaries were washed with 10 ml HBSS at 2500 rpm for 5 min followed by sequential digestions with collagenase (Sigma # C0130, 2ml 1.5 mg/ml collagenase /10 pituitaries) for 2hr at 37 °C and in pancreatin solution (Sigma # P3292, 4.5 mg/ml pancreatin) for 15min at 37 °C. Finally pellets were washed with 10% FBS DMEM followed by centrifugation at 2500 rpm for 5 min. The primary pituitary cells were counted and placed into Matrigel-coated 24-well (cell density is around $0.5X10^6$/well) or 384-well plate ($1.5x10^4$/well) and incubated for 24hr in DMEM-phenol red with 10% FBS, 100U/mL penicillin and 100µg/mL streptomycin using standard methods(65-

68). Cells were then cultured in 1nM and 10nM DHT or vehicle (no DHT) for 42hr. We chose a 42hr DHT incubation time because we observed that DHT inhibited GnRH stimulated LH secretion in cultured primary pituitary cells after 36 to 48 hrs of DHT treatment (data not shown). Cells were incubated with serum free medium without phenol red for 3hr before GnRH stimulation. GnRH was added into medium and media were collected after 2hr treatment. LH and FSH levels were measured by a Luminex assay or an ultrasensitive LH ELISA**.** Treatments were performed in triplicate or quadruplicates and experiments were independently repeated at least three times.

Superovulation and egg retrieval

Female mice at diestrus after 3 weeks of DHT or no-DHT treatment were administered 5IU or 10IU of human chorionic gonadotropin (hCG; cat#C1063-1VL, Sigma, St. Louis, MO, USA) and were euthanized between 14-16h after the hCG injection. The oviducts were collected and the transparent ampulla region of each oviduct was torn open to release the cumulus–oocyte complexes (COCs) into PBS and oocytes were counted.

Inducing LH surges with DHT and estrogen

The mouse surge protocol was adapted from(41,59). Adult female mice were implanted with DHT for 3 days, and on the third day of DHT treatment, mice were ovariectomized (OVX) in the morning, and treated with 50 µl of 17β- estradiol (20ng/µl in sesame oil, Cayman Chemical Company) by injection. On the fourth day (the next day after OVX), blood was collected from each individual OVX mouse by mandibular vein puncture at 10:00 A.M., and 1 h before lights off at 8:00 P.M, and at 9pm. LH levels were measured by a Luminex assay.

Intracellular Calcium Kinetics assay

Mice were treated with a DHT pellet or empty pellet for at least 3 weeks. Pituitaries were isolated at diestrus and primary pituitary cells were cultured in 384-well plates and treated with or without DHT (10nM) for 42h and starved for 3hr before calcium kinetic assay. Calcium dynamics in these cells were measured immediately after treatment with GnRH (10nM or 50 nM) by the Johns Hopkins Chem Core Facility using a modified protocol described previously(69). Briefly,

intracellular calcium signals were detected with BD Calcium Assay Kit (Cat#: 640176, BD Biosciences, San Jose, CA) following manufacturer's instructions. Briefly, 25 µl/well of culture medium were placed in a 384-well plate, the wells were then loaded with 25 µl 1X Dye-loading solution and incubated for 1hr at 37°C. GnRH agonist was added (5 µl/well) by a FlexStation (Molecular Devices) and the kinetic curve of calcium response signals were continuously recorded before and after GnRH addition. Readings (excitation: 480nm; emission: 540 nm) were performed at 1-sec intervals. A fluorescence ratio (480/540 nm ratio) was then calculated.

Ovarian Histology

Ovaries were dissected from mice at diestrus that had been treated with pellets for more than 6 weeks. One ovary was snap frozen in liquid nitrogen for RNA or protein isolation. The other ovary was fixed in 10% formalin phosphate buffer, and the paraffin embedded ovary was sectioned at 5 µm thickness and every 10^{th} section (total of 5 sections) was collected and stained with hematoxylin and eosin (H&E) at the Johns Hopkins Histology Core Facility. Ovaries were examined, and corpora lutea (CLs) were counted with a Zeiss microscope (70).

Androgen binding site prediction and validation with chromatin immunoprecipitation (ChIP)

The regulatory sequence analysis tools (RSAT) web server (http://rsat.ulb.ac.be/rsat/) can predict putative cis-regulatory elements and regions. The approach applies to known transcription factors, whose binding specificity is represented by position-specific scoring matrices, using the program matrix-scan. Androgen response elements (AREs) consist of a 15-bp partially palindromic motif: GGTACAnnnTGTTCT, or containing the core requirement of three (which are underlined) out of four guanines contacts(71). To predict androgen receptor binding sites, we scanned between -5000bp and the transcriptional start site of the *Gem* gene.

To validate the putative androgen receptor binding sites of the *Gem* promoter, Chromatin Immunoprecipitation (ChIP) was performed. Control mice were treated with a DHT pellet or a non-DHT pellet for 3 weeks as described above. The mice were sacrificed and pituitaries were

collected and frozen immediately in liquid nitrogen. ChIP was performed with ChIP-IT® Express Chromatin Immunoprecipitation Kits (Cat# 53008, Active Motif) following the instructions. Anti-Androgen Receptor antibody (Cat#74272; Abcam, Cambridge, MA) and Anti-histone H4 antibody (Cat#: sc-25260; Santa Cruz, Dallas, TX) were used as a positive control in immunoprecipitation. Pituitaries isolated from PitARKO-DHT were used as negative control. qRT-PCR was performed with qPCR kit (Cat# 170-8882, iQTM SYBR Green Supermix, Bio-Rad) following the instructions. Primers are listed in Table 1.

Androgen regulation of Gem promoter luciferase expression

To analyze whether DHT directly regulates *gem* expression, the *Gem* promoter (-3000bp, encompassing the two predicted binding sites in the promoter, the transcription site is referred as position "0" was inserted into PA3-LUC firefly luciferase reporter construct (*Gem*-LUC). TK-Renilla was used as an internal control. Wild type AR plasmid(72) and *Gem*-LUC were co-transfected into 96-well H2.35 cell lines to test the *Gem* promoter activity. DHT was applied to the cells at the doses of 0, 1, 10 or 100nM. Empty vector PA3-LUC (replaced *Gem*-LUC) with the same treatment was used as a basal control. The fold change is expressed as the relative firefly/renilla luciferase values versus its empty vector value (basal control). Three independent experiments were conducted and each one with 4 to 8 replicates.

Statistical analysis

Data were analyzed by an unpaired Student's t test (two-tailed), by one-way ANOVA followed by Tukey's post hoc test, or two-way ANOVA followed by Sidak's multiple comparisons test (specifically addressed in figure legends) accordingly using GraphPad Prism (GraphPad Software). All results are expressed as means ± SEM. Statistical significance was defined as $P<0.05$.

Author contributions

Z.W. and S.W. contributed to the experimental design, conducting the experiments, writing and editing the manuscript. M.F., O.A., Y.M., M.S. and P.X. contributed to performing some of the experiments, analyzing the corresponding data and writing part of the manuscript. J.S., R.A and A.W. contributed to the experimental design and reviewing and editing the manuscript.

Acknowledgments

We thank Dr. Ursula Kaiser (Professor of Medicine, Harvard Medical School) for sharing the pituitary primary cell culture protocols. This work was supported by the National Institutes of Health (Grants R00-HD068130 to S.W.) and the Baltimore Diabetes Research Center: Pilots and Feasibility Grant (to S.W.).

References

1. Lizneva D, Suturina L, Walker W, Brakta S, Gavrilova-Jordan L, Azziz R. Criteria, prevalence, and phenotypes of polycystic ovary syndrome. *Fertil Steril*. 2016;106(1):6-15.

2. Goodarzi MO, Carmina E, Azziz R. DHEA, DHEAS and PCOS. *J Steroid Biochem Mol Biol*. 2015;145:213-225.

3. Carmina E, Dewailly D, Escobar-Morreale HF, et al. Non-classic congenital adrenal hyperplasia due to 21-hydroxylase deficiency revisited: an update with a special focus on adolescent and adult women. *Hum Reprod Update*. 2017;23(5):580-599.

4. van Houten EL, Kramer P, McLuskey A, Karels B, Themmen AP, Visser JA. Reproductive and metabolic phenotype of a mouse model of PCOS. *Endocrinology*. 2012;153(6):2861-2869.

5. Ambroziak U, Kepczynska-Nyk A, Kurylowicz A, et al. The diagnosis of nonclassic congenital adrenal hyperplasia due to 21-hydroxylase deficiency, based on serum basal or post-ACTH stimulation 17-hydroxyprogesterone, can lead to false-positive diagnosis. *Clin Endocrinol (Oxf)*. 2016;84(1):23-29.

6. Chan KJ, Liang JJ, Jolly D, Weinand JD, Safer JD. Exogenous Testosterone does Not Induce Or Exacerbate the Metabolic Features Associated with Pcos among Transgender Men. *Endocr Pract*. 2018.

7. Caanen MR, Soleman RS, Kuijper EA, et al. Antimullerian hormone levels decrease in female-to-male transsexuals using testosterone as cross-sex therapy. *Fertil Steril*. 2015;103(5):1340-1345.

8. Pache TD, Chadha S, Gooren LJ, et al. Ovarian morphology in long-term androgen-treated female to male transsexuals. A human model for the study of polycystic ovarian syndrome? *Histopathology*. 1991;19(5):445-452.

9. Spinder T, Spijkstra JJ, van den Tweel JG, et al. The effects of long term testosterone administration on pulsatile luteinizing hormone secretion and on ovarian histology in eugonadal female to male transsexual subjects. *J Clin Endocrinol Metab*. 1989;69(1):151-157.

10. Bosinski HA, Peter M, Bonatz G, et al. A higher rate of hyperandrogenic disorders in female-to-male transsexuals. *Psychoneuroendocrinology*. 1997;22(5):361-380.

11. Diamanti-Kandarakis E, Bourguignon JP, Giudice LC, et al. Endocrine-disrupting chemicals: an Endocrine Society scientific statement. *Endocr Rev*. 2009;30(4):293-342.

12. Caldwell AS, Middleton LJ, Jimenez M, et al. Characterization of reproductive, metabolic, and endocrine features of polycystic ovary syndrome in female hyperandrogenic mouse models. *Endocrinology*. 2014;155(8):3146-3159.

13. Kauffman AS, Thackray VG, Ryan GE, et al. A Novel Letrozole Model Recapitulates Both the Reproductive and Metabolic Phenotypes of Polycystic Ovary Syndrome in Female Mice. *Biol Reprod*. 2015;93(3):69.

14. Kelley ST, Skarra DV, Rivera AJ, Thackray VG. The Gut Microbiome Is Altered in a Letrozole-Induced Mouse Model of Polycystic Ovary Syndrome. *PLoS One*. 2016;11(1):e0146509.

15. Kafali H, Iriadam M, Ozardali I, Demir N. Letrozole-induced polycystic ovaries in the rat: a new model for cystic ovarian disease. *Arch Med Res*. 2004;35(2):103-108.

16. Cardoso RC, Puttabyatappa M, Padmanabhan V. Steroidogenic versus Metabolic Programming of Reproductive Neuroendocrine, Ovarian and Metabolic Dysfunctions. *Neuroendocrinology*. 2015;102(3):226-237.

17. Dumesic DA, Abbott DH, Padmanabhan V. Polycystic ovary syndrome and its developmental origins. *Rev Endocr Metab Disord*. 2007;8(2):127-141.

18. De Leo V, Lanzetta D, D'Antona D, la Marca A, Morgante G. Hormonal effects of flutamide in young women with polycystic ovary syndrome. *J Clin Endocrinol Metab*. 1998;83(1):99-102.

19. Brothers KJ, Wu S, DiVall SA, et al. Rescue of obesity-induced infertility in female mice due to a pituitary-specific knockout of the insulin receptor. *Cell Metab*. 2010;12(3):295-305.

20. Delemarre-van de Waal HA, van Coeverden SC, Engelbregt MT. Factors affecting onset of puberty. *Horm Res*. 2002;57 Suppl 2:15-18.

21. Andrisse S, Childress S, Ma Y, et al. Low Dose Dihydrotestosterone Drives Metabolic Dysfunction via Cytosolic and Nuclear Hepatic Androgen Receptor Mechanisms. *Endocrinology*. 2016:en20161553.

22. Ma Y, Andrisse S, Chen Y, et al. Androgen Receptor in the Ovary Theca Cells Plays a Critical Role in Androgen-Induced Reproductive Dysfunction. *Endocrinology*. 2016:en20161608.

23. Xue P, Wang Z, Fu X, et al. A Hyperandrogenic Mouse Model to Study Polycystic Ovary Syndrome. *J Vis Exp*. 2018;(140). doi(140):10.3791/58379.

24. Silfen ME, Denburg MR, Manibo AM, et al. Early endocrine, metabolic, and sonographic characteristics of polycystic ovary syndrome (PCOS): comparison between nonobese and obese adolescents. *J Clin Endocrinol Metab*. 2003;88(10):4682-4688.

581 25. Fassnacht M, Schlenz N, Schneider SB, Wudy SA, Allolio B, Arlt W. Beyond adrenal and
582 ovarian androgen generation: Increased peripheral 5 alpha-reductase activity in women with
583 polycystic ovary syndrome. *J Clin Endocrinol Metab*. 2003;88(6):2760-2766.

584 26. Eden JA, Jones J, Carter GD, Alaghband-Zadeh J. Follicular fluid concentrations of insulin-
585 like growth factor 1, epidermal growth factor, transforming growth factor-alpha and sex-steroids
586 in volume matched normal and polycystic human follicles. *Clin Endocrinol (Oxf)*.
587 1990;32(4):395-405.

588 27. Qu F, Wang FF, Lu XE, et al. Altered aquaporin expression in women with polycystic ovary
589 syndrome: hyperandrogenism in follicular fluid inhibits aquaporin-9 in granulosa cells through
590 the phosphatidylinositol 3-kinase pathway. *Hum Reprod*. 2010;25(6):1441-1450.

591 28. Nakamura Y, Yoshimura Y, Kamei K, Izumi Y, Sawada T, Iizuka R. Androgen production by
592 human isolated components of normal and polycystic ovaries in vitro. *Endocrinol Jpn*.
593 1982;29(3):307-317.

594 29. Wickenheisser JK, Nelson-DeGrave VL, Hendricks KL, Legro RS, Strauss JF,3rd, McAllister
595 JM. Retinoids and retinol differentially regulate steroid biosynthesis in ovarian theca cells
596 isolated from normal cycling women and women with polycystic ovary syndrome. *J Clin*
597 *Endocrinol Metab*. 2005;90(8):4858-4865.

598 30. de Resende LO, dos Reis RM, Ferriani RA, et al. Concentration of steroid hormones in the
599 follicular fluid of mature and immature ovarian follicles of patients with polycystic ovary
600 syndrome submitted to in vitro fertilization. *Rev Bras Ginecol Obstet*. 2010;32(9):447-453.

601 31. Andrisse S, Billings K, Xue P, Wu S. Insulin signaling displayed a differential tissue-specific
602 response to low-dose dihydrotestosterone in female mice. *Am J Physiol Endocrinol Metab*.
603 2018;314(4):E353-E365.

604 32. Caldwell ASL, Edwards MC, Desai R, et al. Neuroendocrine androgen action is a key
605 extraovarian mediator in the development of polycystic ovary syndrome. *Proc Natl Acad Sci U S*
606 *A*. 2017;114(16):E3334-E3343.

607 33. Silva MS, Prescott M, Campbell RE. Ontogeny and reversal of brain circuit abnormalities in
608 a preclinical model of PCOS. *JCI Insight*. 2018;3(7):10.1172/jci.insight.99405.

609 34. Wu S, Chen Y, Fajobi T, et al. Conditional knockout of the androgen receptor in
610 gonadotropes reveals crucial roles for androgen in gonadotropin synthesis and surge in female
611 mice. *Mol Endocrinol*. 2014;28(10):1670-1681.

612 35. Kamel F, Krey LC. Gonadal steroid modulation of LHRH-stimulated LH secretion by pituitary
613 cell cultures. *Mol Cell Endocrinol*. 1982;26(1-2):151-164.

614 36. Beguin P, Nagashima K, Gonoi T, et al. Regulation of Ca2+ channel expression at the cell
615 surface by the small G-protein kir/Gem. *Nature*. 2001;411(6838):701-706.

616 37. Melamed P, Savulescu D, Lim S, et al. Gonadotrophin-releasing hormone signalling
617 downstream of calmodulin. *J Neuroendocrinol*. 2012;24(12):1463-1475.

618 38. Correll RN, Pang C, Niedowicz DM, Finlin BS, Andres DA. The RGK family of GTP-binding
619 proteins: regulators of voltage-dependent calcium channels and cytoskeleton remodeling. *Cell*
620 *Signal*. 2008;20(2):292-300.

621 39. Stefaneanu L. Pituitary Sex Steroid Receptors: Localization and Function. *Endocr Pathol*.
622 1997;8(2):91-108.

623 40. Yuan X, He Y, Liu J, Luo H, Zhang J, Cui S. Expression of androgen receptor and its co-
624 localization with estrogen receptor-alpha in the developing pituitary gland of sheep fetus.
625 *Histochem Cell Biol*. 2007;127(4):423-432.

626 41. Foecking EM, Levine JE. Effects of experimental hyperandrogenemia on the female rat
627 reproductive axis: suppression of progesterone-receptor messenger RNA expression in the
628 brain and blockade of luteinizing hormone surges. *Gend Med*. 2005;2(3):155-165.

629 42. Foecking EM, McDevitt MA, Acosta-Martinez M, Horton TH, Levine JE. Neuroendocrine
630 consequences of androgen excess in female rodents. *Horm Behav*. 2008;53(5):673-692.

631 43. Iwata K, Kunimura Y, Matsumoto K, Ozawa H. Effect of androgen on Kiss1 expression and
632 luteinizing hormone release in female rats. *J Endocrinol*. 2017;233(3):281-292.

633 44. Santen RJ. Is aromatization of testosterone to estradiol required for inhibition of luteinizing
634 hormone secretion in men? *J Clin Invest*. 1975;56(6):1555-1563.

635 45. Marynick SP, Loriaux DL, Sherins RJ, Pita JC,Jr, Lipsett MB. Evidence that testosterone
636 can suppress pituitary gonadotropin secretion independently of peripheral aromatization. *J Clin*
637 *Endocrinol Metab*. 1979;49(3):396-398.

638 46. Moore AM, Campbell RE. Polycystic ovary syndrome: Understanding the role of the brain.
639 *Front Neuroendocrinol*. 2017;46:1-14.

47. Eagleson CA, Gingrich MB, Pastor CL, et al. Polycystic ovarian syndrome: evidence that flutamide restores sensitivity of the gonadotropin-releasing hormone pulse generator to inhibition by estradiol and progesterone. *J Clin Endocrinol Metab*. 2000;85(11):4047-4052.

48. Goodman NF, Cobin RH, Futterweit W, et al. American Association of Clinical Endocrinologists, American College of Endocrinology, and Androgen Excess and Pcos Society Disease State Clinical Review: Guide to the Best Practices in the Evaluation and Treatment of Polycystic Ovary Syndrome - Part 2. *Endocr Pract*. 2015;21(12):1415-1426.

49. Diamanti-Kandarakis E, Mitrakou A, Raptis S, Tolis G, Duleba AJ. The effect of a pure antiandrogen receptor blocker, flutamide, on the lipid profile in the polycystic ovary syndrome. *J Clin Endocrinol Metab*. 1998;83(8):2699-2705.

50. Blank SK, McCartney CR, Marshall JC. The origins and sequelae of abnormal neuroendocrine function in polycystic ovary syndrome. *Hum Reprod Update*. 2006;12(4):351-361.

51. Ryan GE, Malik S, Mellon PL. Antiandrogen Treatment Ameliorates Reproductive and Metabolic Phenotypes in the Letrozole-Induced Mouse Model of PCOS. *Endocrinology*. 2018;159(4):1734-1747.

52. Goodarzi MO, Dumesic DA, Chazenbalk G, Azziz R. Polycystic ovary syndrome: etiology, pathogenesis and diagnosis. *Nat Rev Endocrinol*. 2011;7(4):219-231.

53. Shorakae S, Boyle J, Teede H. Polycystic ovary syndrome: a common hormonal condition with major metabolic sequelae that physicians should know about. *Intern Med J*. 2014;44(8):720-726.

661 54. Walters KA. Role of androgens in normal and pathological ovarian function. *Reproduction*.
662 2015;149(4):R193-218.

663 55. Yasin M, Dalkin AC, Haisenleder DJ, Marshall JC. Testosterone is required for
664 gonadotropin-releasing hormone stimulation of luteinizing hormone-beta messenger ribonucleic
665 acid expression in female rats. *Endocrinology*. 1996;137(4):1265-1271.

666 56. Silfen ME, Denburg MR, Manibo AM, et al. Early endocrine, metabolic, and sonographic
667 characteristics of polycystic ovary syndrome (PCOS): comparison between nonobese and
668 obese adolescents. *J Clin Endocrinol Metab*. 2003;88(10):4682-4688.

669 57. Fassnacht M, Schlenz N, Schneider SB, Wudy SA, Allolio B, Arlt W. Beyond adrenal and
670 ovarian androgen generation: Increased peripheral 5 alpha-reductase activity in women with
671 polycystic ovary syndrome. *J Clin Endocrinol Metab*. 2003;88(6):2760-2766.

672 58. Caldwell AS, Eid S, Kay CR, et al. Haplosufficient genomic androgen receptor signaling is
673 adequate to protect female mice from induction of polycystic ovary syndrome features by
674 prenatal hyperandrogenization. *Endocrinology*. 2015;156(4):1441-1452.

675 59. Wu S, Divall S, Hoffman GE, Le WW, Wagner KU, Wolfe A. Jak2 is necessary for
676 neuroendocrine control of female reproduction. *J Neurosci*. 2011;31(1):184-192.

677 60. Stojilkovic SS. Pituitary cell type-specific electrical activity, calcium signaling and secretion.
678 *Biol Res*. 2006;39(3):403-423.

679 61. Stojilkovic SS, Stutzin A, Izumi S, et al. Generation and amplification of the cytosolic calcium
680 signal during secretory responses to gonadotropin-releasing hormone. *New Biol*. 1990;2(3):272-
681 283.

62. Ortmann O, Tomic M, Weiss JM, Diedrich K, Stojilkovic SS. Dual action of androgen on calcium signaling and luteinizing hormone secretion in pituitary gonadotrophs. *Cell Calcium*. 1998;24(3):223-231.

63. Wang Z, Shen M, Xue P, DiVall SA, Segars J, Wu S. Female Offspring From Chronic Hyperandrogenemic Dams Exhibit Delayed Puberty and Impaired Ovarian Reserve. *Endocrinology*. 2018;159(2):1242-1252.

64. Nelson JF, Felicio LS, Randall PK, Sims C, Finch CE. A longitudinal study of estrous cyclicity in aging C57BL/6J mice: I. Cycle frequency, length and vaginal cytology. *Biol Reprod*. 1982;27(2):327-339.

65. Krey LC, Kamel F. Progesterone modulation of gonadotropin secretion by dispersed rat pituitary cells in culture. I. Basal and gonadotropin-releasing hormone-stimulated luteinizing hormone release. *Mol Cell Endocrinol*. 1990;68(2-3):85-94.

66. Savulescu D, Feng J, Ping YS, et al. Gonadotropin-releasing hormone-regulated prohibitin mediates apoptosis of the gonadotrope cells. *Mol Endocrinol*. 2013;27(11):1856-1870.

67. Wen S, Schwarz JR, Niculescu D, et al. Functional characterization of genetically labeled gonadotropes. *Endocrinology*. 2008;149(6):2701-2711.

68. Do MH, Santos SJ, Lawson MA. GNRH induces the unfolded protein response in the LbetaT2 pituitary gonadotrope cell line. *Mol Endocrinol*. 2009;23(1):100-112.

69. Song WJ, Mondal P, Li Y, Lee SE, Hussain MA. Pancreatic beta-cell response to increased metabolic demand and to pharmacologic secretagogues requires EPAC2A. *Diabetes*. 2013;62(8):2796-2807.

703 70. Wu S, Divall S, Nwaopara A, et al. Obesity-induced infertility and hyperandrogenism are
704 corrected by deletion of the insulin receptor in the ovarian theca cell. *Diabetes*.
705 2014;63(4):1270-1282.

706 71. Claessens F, Verrijdt G, Schoenmakers E, et al. Selective DNA binding by the androgen
707 receptor as a mechanism for hormone-specific gene regulation. *J Steroid Biochem Mol Biol*.
708 2001;76(1-5):23-30.

709 72. Yu IC, Lin HY, Liu NC, et al. Neuronal androgen receptor regulates insulin sensitivity via
710 suppression of hypothalamic NF-kappaB-mediated PTP1B expression. *Diabetes*.
711 2013;62(2):411-423.

712
713
714
715
716
717
718
719
720
721
722
723
724
725
726
727
728

Figure Legends:

Figure 1. Overview of mouse models used in this study to elucidate the role of AR in gonadotropes in androgen excess.

Figure 2. Estrous cyclicity. Murine estrous cyclicity was examined by vaginal smear. A. The examples of estrous cyclicity in each group. (P=proestrus; E=estrus; M/D=Metestrus/Diestrus). B. The percentage time in each stage was calculated by the total days of each estrous stage divided by the total number (16) of days. N= 6-30. Data were compared by two tailed student t-test. P values are indicated as *=P<0.05; NS=No significant difference.

Figure 3. Fertility assessment. A. Female mice were mated with proven fertile male mouse for 90 days, and the number of litters and pups were recorded. Plots of mating outcomes for Con-DHT (top) and PitARKO-DHT mice (bottom). Each line represents an individual female mouse, black dot represents the day that each litter was born after introduction to male, and number above each line represents number of pups per litter. B. Number of litters per female. C. Number of pups per female. N=6-9 females/group. Data were compared by two-way ANOVA followed by Sidak's multiple comparisons test. Different letters represent significant difference. D-G. Ovary histology. Ovary was sectioned and H&E stained. Representative sections of ovaries from Con-no DHT, PitARKO-no DHT, Con-DHT, PitARKO-DHT. CL = corpora lutea. H. Quantitative analysis of CL number. CLs were recorded in each group of ovaries. N=6-19 mice. Open bars, vehicle treated, black bars, DHT treated. Data were compared by two tailed student t-test. P values are indicated as *=P<0.05; ***=P<0.0001; NS=No significant difference.

Figure 4. Pituitary hormone secretion and gene expression. A. Serum LH levels and B. FSH levels before (basal) and after GnRH stimulation in vivo. Open bars, vehicle treated, black bars, DHT treated. NS= no significant difference. N=5-10. Data were compared by two-tailed student t-test. C-D. LH and FSH secretion (3 independent experiments) from cell culture of pooled primary pituitaries (ng/ml). N=3 (3-5 pituitaries/pool/experiment, total number of pituitaries=9-15). Data with and without GnRH stimulation were compared separately by one-way ANOVA followed by Tukey's post hoc test. E-I. Pituitary gene expression. E-F. Ex vivo experiments. *Lhβ* and *Gem* mRNA levels after DHT treatment in primary pituitary cell culture. Open bar is vehicle-treated, shaded bars are DHT treated at the indicated concentration. Data were compared by One-Way ANOVA followed by Tukey's post hoc test. N=4. Different letters represent significant difference. G-I. In vivo experiments. Pituitaries were isolated from female mice at diestrus after 7-10 weeks pellet insertion. G. *Ar*; H. *Lhβ*, I. *Gem* mRNA displayed as relative fold to Con-No DHT. N=4-6 mice per group. Data were compared by two-tailed student t-test. * =$p<0.05$; **=$p<0.01$; ***=$p<0.001$; NS=not significant.

Figure 5. A-B. Long term DHT treatment impaired calcium signaling of pituitary Cells in response to GnRH. Pooled primary pituitary cell cultures from 3-5 mice were treated with vehicle or DHT pellet for 6 weeks (in vivo) were incubated ex vivo with or without DHT for 42h before treating with 50nM GnRH. Intracellular calcium signaling was immediately measured. Fura-2/Ca2+-specific signals were captured and 480/540 nm ratio calculated for Con-GnRH, PitARK-GnRH, Con-DHT-GnRH, and PitARKO-DHT-GnRH groups. N=4 independent experiments (total 12-20 pituitaries). C-F. ChIP assay. C. Primer sets were designed flanking the AR consensus binding site (BS) position 1 (with primers 45 and 46) and 2 (with primers 47 and 48) in the Gem promoter. D-E. CHIP assay was performed with 3-5 pooled pituitaries using antibody to AR and anti-H4. qRT-PCR was conducted with primers flanking the Gem promoter binding site 1 and 2. Results were normalized to input from 3 independent ChIP experiments.

N=3 (9-15 pituitaries). F. qRT- PCR data of AR binding to the Gem promoter with negative control (PitARKO-DHT) was shown (for primer set 45 and 46) in a 1.5% agarose gel as a representative example. G. DHT increased Gem promoter expression. The Gem promoter was inserted into a luciferase reporter and the relative fold was shown as luciferase data divided its internal control of renilla and its own empty vector under the same treatment. N=3 independent experiments. Each individual experiment was conducted with 4 to 8 replicates. Data from B, D, E were compared by two-tailed student t-test. Data from G were compared by one-way ANOVA followed by Tukey's post hoc test. Different letters represent significant difference.

Figure 6. Working model. We hypothesize that in the presence of androgen excess, androgen/AR binds to DHT helping assemble active transcription machinery on the promoter of Gem and increasing Gem mRNA level. GEM inhibits calcium influx by blocking voltage-dependent calcium channel (VDCC). GnRH binds its receptor (GnRHR) to induce release of LH by stimulating vesicle exocytosis. Reduced cytosolic Ca2+ concentration due to increased GEM inhibits Ca2+ triggered exocytosis, reducing LH vesicle secretion during GnRH stimulation. ER: endoplasmic reticulum.

806

807

808

809

810

Table 1

Primers for qRT-PCR

Ihb	F	GGCCGCAGAGAATGAGTTCTG
	R	CTGAGGCACAGGAGGCAAA
Ar	F	GGCGGTCCTTCACTAATGTCAACT
	R	GAGACTTGTGCATGCGGTACTCAT
Gem	F	AAATCCTGCCATGACCTGTC
	R	GGAAGTTGCGTCTAACAATGC
Gem promoter	F45	GGTTCTGAG ATGCGCTGA T
	R46	GCAGCTTGTGCTAAACAGTG
Gem promoter	F47	TACTCTTTCCTCCGACTCTTC T
	R48	TTCCTGCTTCCTGACTTCTTATC
Gapdh	F	GGG CAT CTT GGG CTA CAC T
	R	GGC ATC GAA GGT GGA AGA GT

811

Figure 1

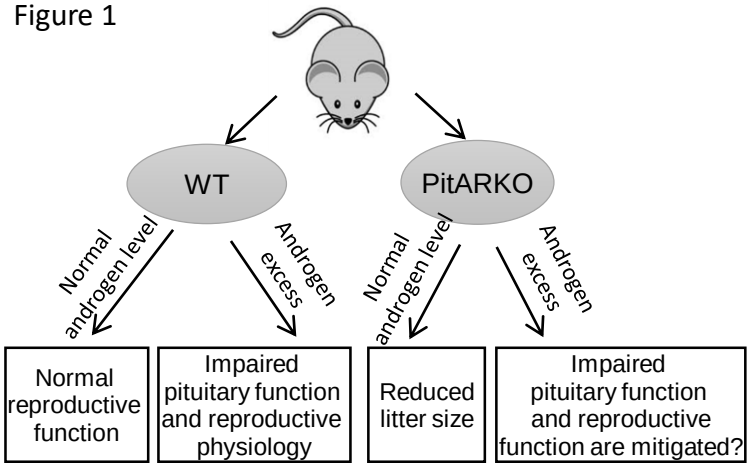

Figure 1. Overview of mouse models used in this study to elucidate the role of AR in gonadotropes in androgen excess.

Figure 2

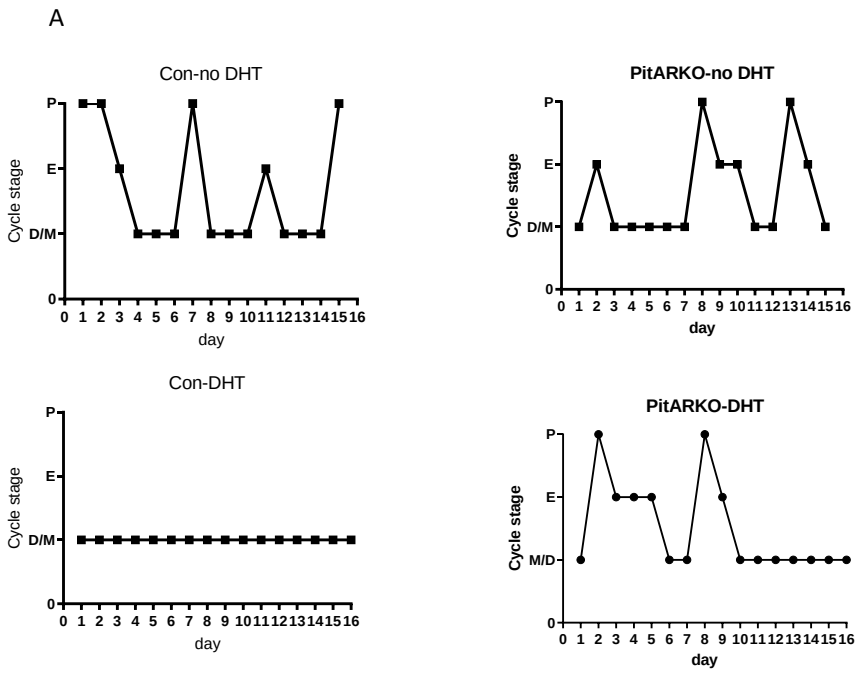

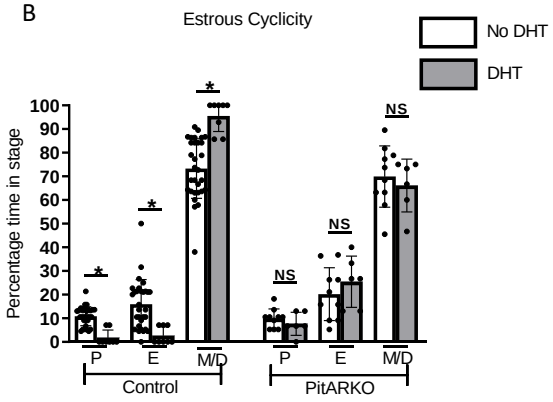

Figure 2. Estrous cyclicity. Murine estrous cyclicity was examined by vaginal smear. A. The examples of estrous cyclicity in each group. (P=proestrus; E=estrus; M/D=Metestrus/Diestrus). B. The percentage time in each stage was calculated by the total days of each estrous stage divided by the total number (16) of days. N= 6-30. Data were compared by two tailed student t-test. P values are indicated as *=P<0.05; NS=No significant difference.

Figure 3

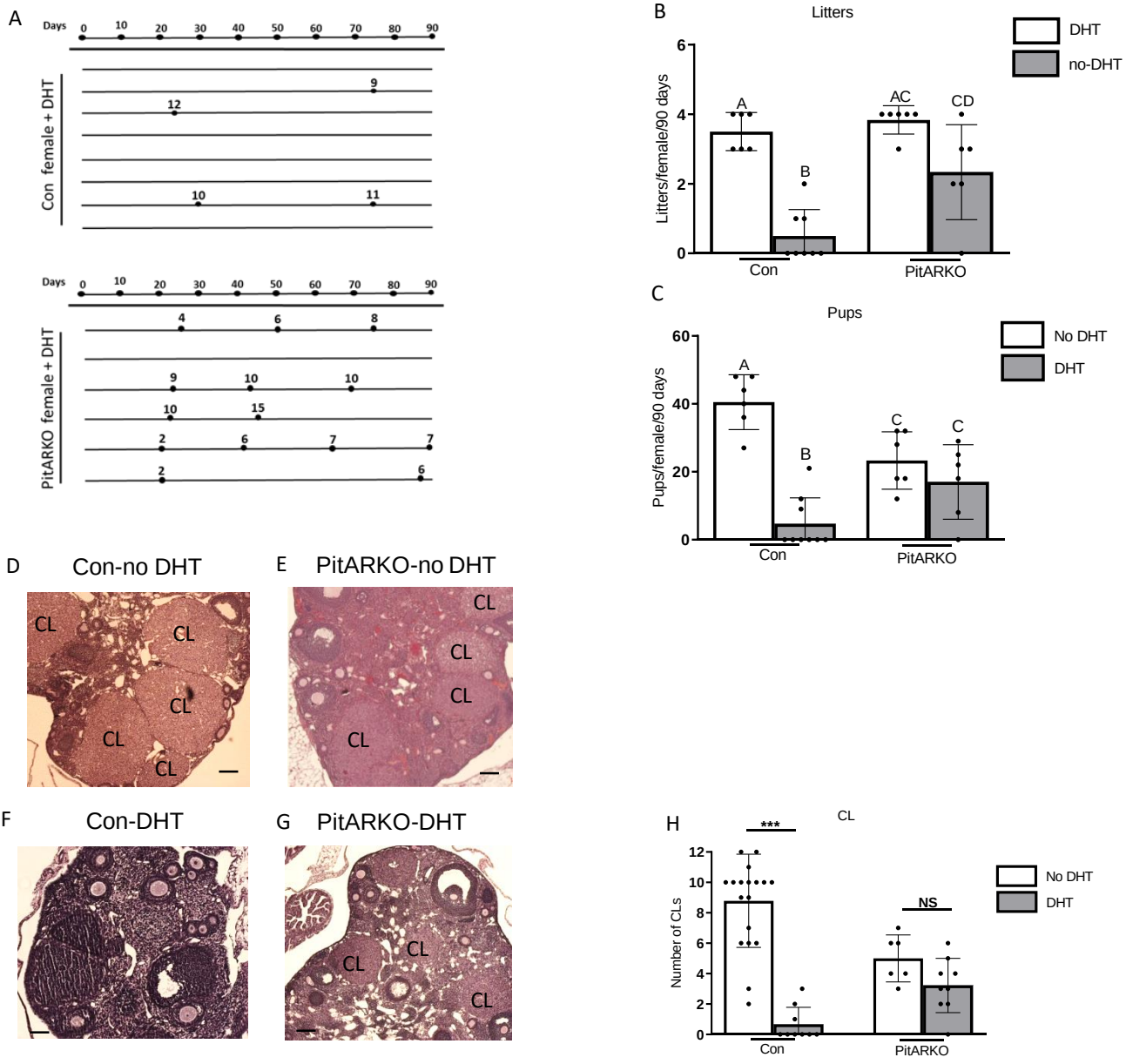

Figure 3. Fertility assessment. A. Female mice were mated with proven fertile male mouse for 90 days, and the number of litters and pups were recorded. Plots of mating outcomes for Con-DHT (top) and PitARKO-DHT mice (bottom). Each line represents an individual female mouse, black dot represents the day that each litter was born after introduction to male, and number above each line represents number of pups per litter. B. Number of litters per female. C. Number of pups per female. N=6-9 females/group. Data were compared by two-way ANOVA followed by Sidak's multiple comparisons test. Different letters represent significant difference. D-G. Ovary histology. Ovary was sectioned and H&E stained. Representative sections of ovaries from Con-no DHT, PitARKO-no DHT, Con-DHT, PitARKO-DHT. CL = corpora lutea. H. Quantitative analysis of CL number. CLs were recorded in each group of ovaries. N=6-19 mice. Open bars, vehicle treated, black bars, DHT treated. Data were compared by two tailed student t-test. P values are indicated as *=P<0.05; ***=P<0.0001; NS=No significant difference.

Figure 4

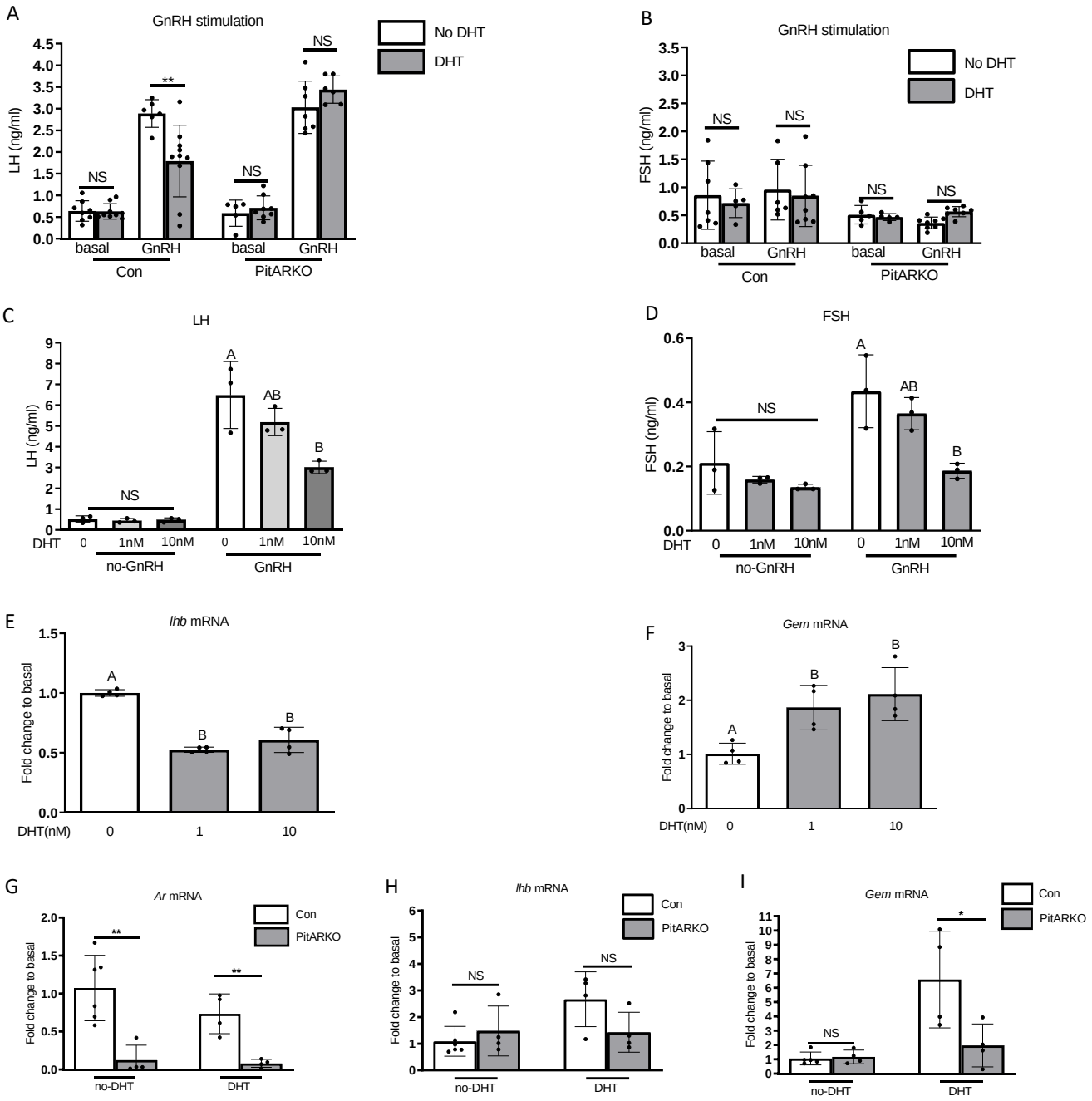

Figure 4. Pituitary hormone secretion and gene expression. A. Serum LH levels and B. FSH levels before (basal) and after GnRH stimulation *in vivo*. Open bars, vehicle treated, black bars, DHT treated. NS= no significant difference. N=5-10. Data were compared by two-tailed student t-test. C-D. LH and FSH secretion (3 independent experiments) from cell culture of pooled primary pituitaries (ng/ml). Data with and without GnRH stimulation were compared separately by one-way ANOVA followed by Tukey's post hoc test. N=3 (total number of pituitaries=9-15). E-I. Pituitary gene expression. E-F. *Ex vivo* experiments. *Lhβ* and *Gem* mRNA levels after DHT treatment in primary pituitary cell culture. Open bar is vehicle-treated, shaded bars are DHT treated at the indicated concentration. Data were compared by One-Way ANOVA followed by Tukey's post hoc test. Different letters represent significant difference. N=4. G-I. *In vivo* experiments. Pituitaries were isolated from female mice at diestrus after 7-10 weeks pellet insertion. G. *Ar*; H. *Lhβ*, I. *Gem* mRNA displayed as relative fold to Con-No DHT. N=4-6 mice per group. Data were compared by two-tailed student t-test. * =p<0.05; **=p<0.01; ***=p<0.001; NS=not significant.

Figure 5

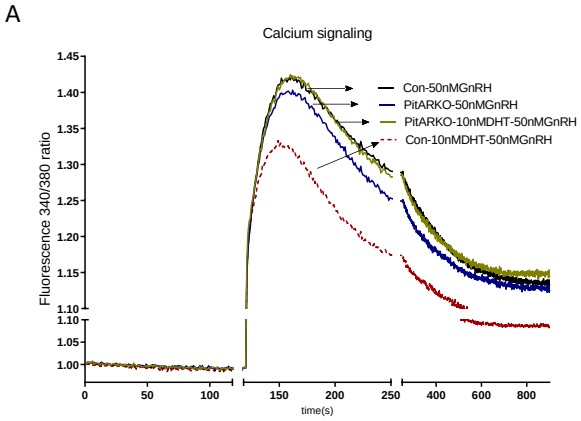

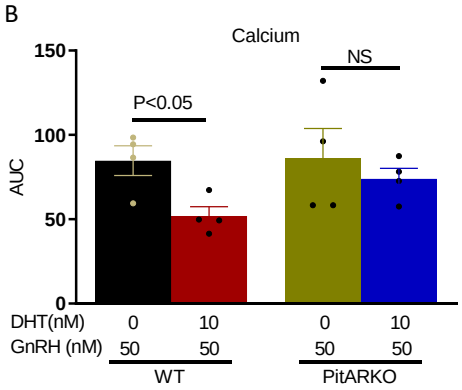

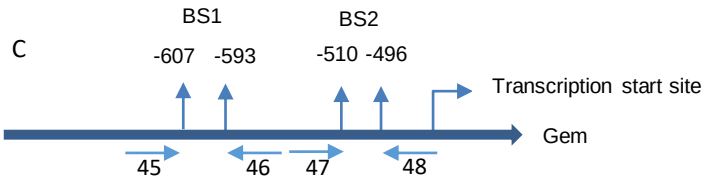

For binding site 1: tagcacaagctgctt; 2 : tgggacatactgctt

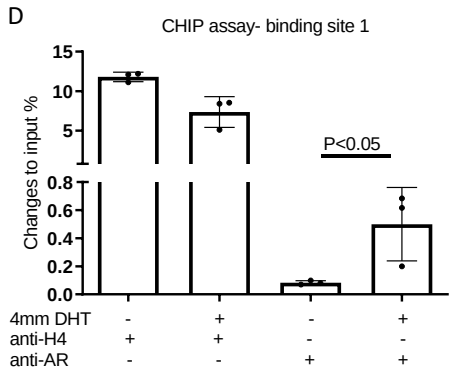

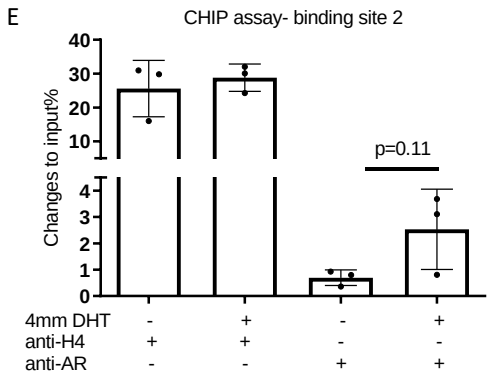

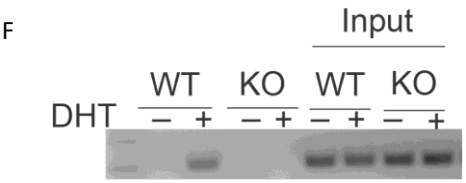

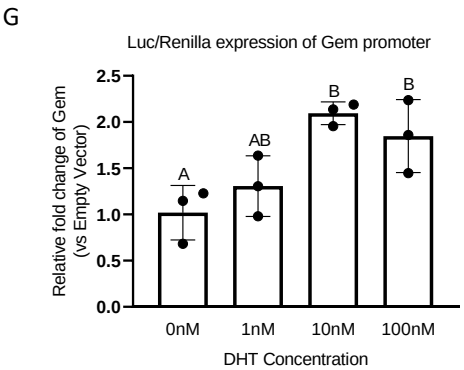

Figure 5. A-B. Long term DHT treatment impaired calcium signaling of pituitary Cells in response to GnRH. Pooled primary pituitary cell cultures from 3-5 mice were treated with vehicle or DHT pellet for 6 weeks (*in vivo*) were incubated *ex vivo* with or without DHT for 42h before treating with 50nM GnRH. Intracellular calcium signaling was immediately measured. Fura-2/Ca2+-specific signals were captured and 480/540 nm ratio calculated for Con-GnRH, PitARK-GnRH, Con-DHT-GnRH, and PitARKO-DHT-GnRH groups. N=4 independent experiments (total 12-20 pituitaries). C-F. ChIP assay. C. Primer sets were designed flanking the AR consensus binding site (BS) position 1 (with primers 45 and 46) and 2 (with primers 47 and 48) in the *Gem* promoter. D-E. CHIP assay was performed with 3-5 pooled pituitaries using antibody to AR and anti-H4. qRT-PCR was conducted with primers flanking the *Gem* promoter binding site 1 and 2. Results were normalized to input from 3 independent ChIP experiments. N=3 (9-15 pituitaries). F. qRT- PCR data of AR binding to the *Gem* promoter with negative control (PitARKO-DHT) was shown (for primer set 45 and 46) in a 1.5% agarose gel as a representative example. G. DHT increased *Gem* promoter expression. The *Gem* promoter was inserted into a luciferase reporter and the relative fold was shown as luciferase data divided its internal control of renilla and its own empty vector under the same treatment. N=3 independent experiments. Each individual experiment was conducted with 4 to 8 replicates. Data from B, D, E were compared by two-tailed student t-test. Data from G were compared by one-way ANOVA followed by Tukey's multiple comparisons test. Different letters represent significant difference.

Figure 6

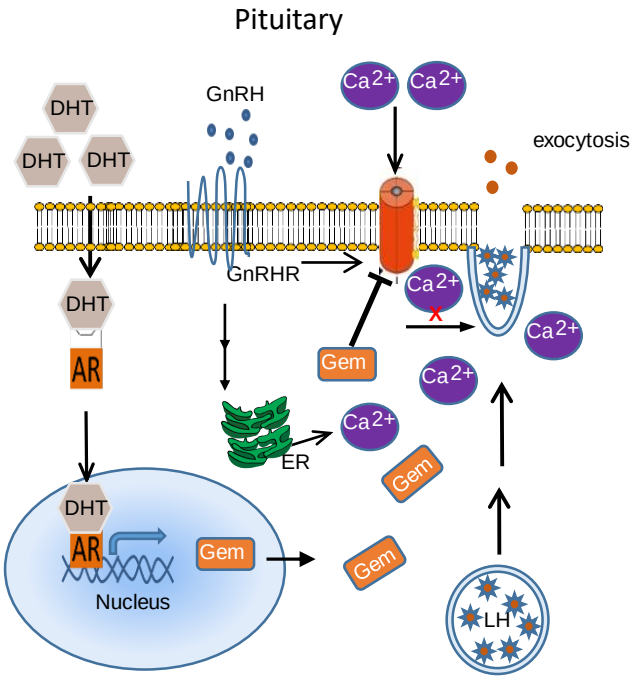

Figure 6. Working model. We hypothesize that in the presence of androgen excess, AR binds to DHT helping assemble active transcription machinery on the promoter of Gem and increasing Gem mRNA level. GEM inhibits calcium influx by blocking voltage-dependent calcium channel (VDCC). GnRH binds its receptor (GnRHR) to induce release of LH by stimulating vesicle exocytosis. Reduced cytosolic Ca2+ concentration due to increased GEM inhibits Ca2+ triggered exocytosis, reducing LH vesicle secretion during GnRH stimulation. ER: endoplasmic reticulum.